ACS chemical biology

Articles

pubs.acs.org/acschemicalbiology

Affinity Profiling of the Cellular Kinome for the Nucleotide Cofactors ATP, ADP, and GTP

Isabelle Becher, Mikhail M. Savitski, Maria Fälth Savitski, Carsten Hopf, Marcus Bantscheff,* and Gerard Drewes*

Cellzome GmbH, Meyerhofstrasse 1, D-69117 Heidelberg, Germany

Supporting Information

ABSTRACT: Most kinase inhibitor drugs target the binding site of the nucleotide cosubstrate ATP. The high intracellular concentration of ATP can strongly affect inhibitor potency and selectivity depending on the affinity of the target kinase for ATP. Here we used a defined chemoproteomics system based on competition-binding assays in cell extracts from Jurkat and SK-MEL-28 cells with immobilized ATP mimetics (kinobeads). This system enabled us to assess the affinities of more than 200 kinases for the cellular nucleotide cofactors ATP, ADP, and GTP and the effects of the divalent metal ions Mg^{2+} and Mn^{2+}. The affinity values determined in this system were largely consistent across the two cell lines, indicating no major dependence on kinase expression levels. Kinase-ATP affinities range from low micromolar to millimolar, which has profound consequences for the prediction of cellular effects from inhibitor selectivity profiles. Only a small number of kinases including CK2, MEK, and BRAF exhibited affinity for GTP. This extensive and consistent data set of kinase-nucleotide affinities, determined for native enzymes under defined experimental conditions, will represent a useful resource for kinase drug discovery.

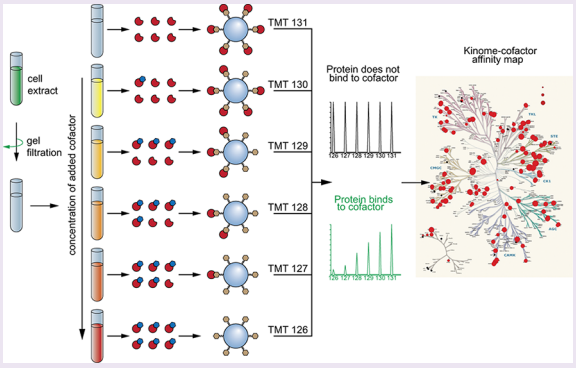

Protein kinases are the largest enzyme family in mammals, and the human kinome represents a major source of drug targets.[1−3] As of 2012, 15 small molecule kinase inhibitors have been approved for human therapy, all for treatment of hematological malignancies or solid tumors.[4−6] About 150 kinase-targeted compounds are in clinical trials, also for indications outside oncology, such as the JAK inhibitors for autoimmune diseases.[7] With the exception of the macrolides that inhibit mTOR, all marketed kinase drugs and the majority of compounds under clinical evaluation target the binding site of the cosubstrate adenosine triphosphate (ATP). This fact implies several hurdles for the discovery of ATP-competitive inhibitors with respect to selectivity and potency. The high degree of structural conservation across ATP-binding sites poses a challenge for kinase inhibitor selectivity,[8] and indeed the majority of current clinical compounds exhibit polypharmacology, *i.e.*, they act *via* the inhibition of several distinct targets.[9,10] Moreover, the high intracellular concentration of ATP, in the low millimolar range,[11,12] together with typical kinase K_M values for ATP in the midmicromolar range, indicates that inhibitors will have to overcome competition by ATP, causing a drop in cellular potency.[13] This leads to a number of practical considerations for kinase drug discovery: compounds that target kinases displaying a low ATP affinity (*i.e.*, high K_M) will show a less pronounced drop in potency between biochemical and cell-based assays. Such kinases might pose less of a challenge for inhibitor discovery, while at the same time they may be underestimated as off-targets in selectivity profiles, in particular if the primary target exhibits high ATP affinity. Incorrect or incomplete assessment of cellular selectivity substantially increases the risk of unexpected toxicities at later stages in drug development that are frequently encountered in kinase inhibitor development.[5,14]

Kinase assay panels for selectivity profiling are an important tool in kinase drug discovery to assess the potential of a compound for off-target liabilities.[10,15−21] However, differences in ATP affinity between different kinases are often not taken into account when analyzing these profiles. A publicly available, consistent data set of kinase K_M or K_D values for ATP, determined under a defined set of experimental conditions, does not exist currently. This is likely due to the different requirements and issues with kinase assays, such as enzyme construct and quality, buffer conditions, and assay design, *e.g.*, enzymatic *versus* binding assays.[13,22] For the same reasons, inhibition data generated with recombinant purified enzymes frequently deviate between different sources. Recent proteomics-based experimental strategies for affinity profiling of small molecules in cell extracts overcome many of these problems and have efficiently enabled the profiling of small molecule affinities across a large number of native endogenous enzyme targets.[23−26] In the present study, we employ a refined adaptation of our "kinobeads" methodology[9,27] to determine

Received: October 29, 2012
Accepted: December 5, 2012
Published: December 5, 2012

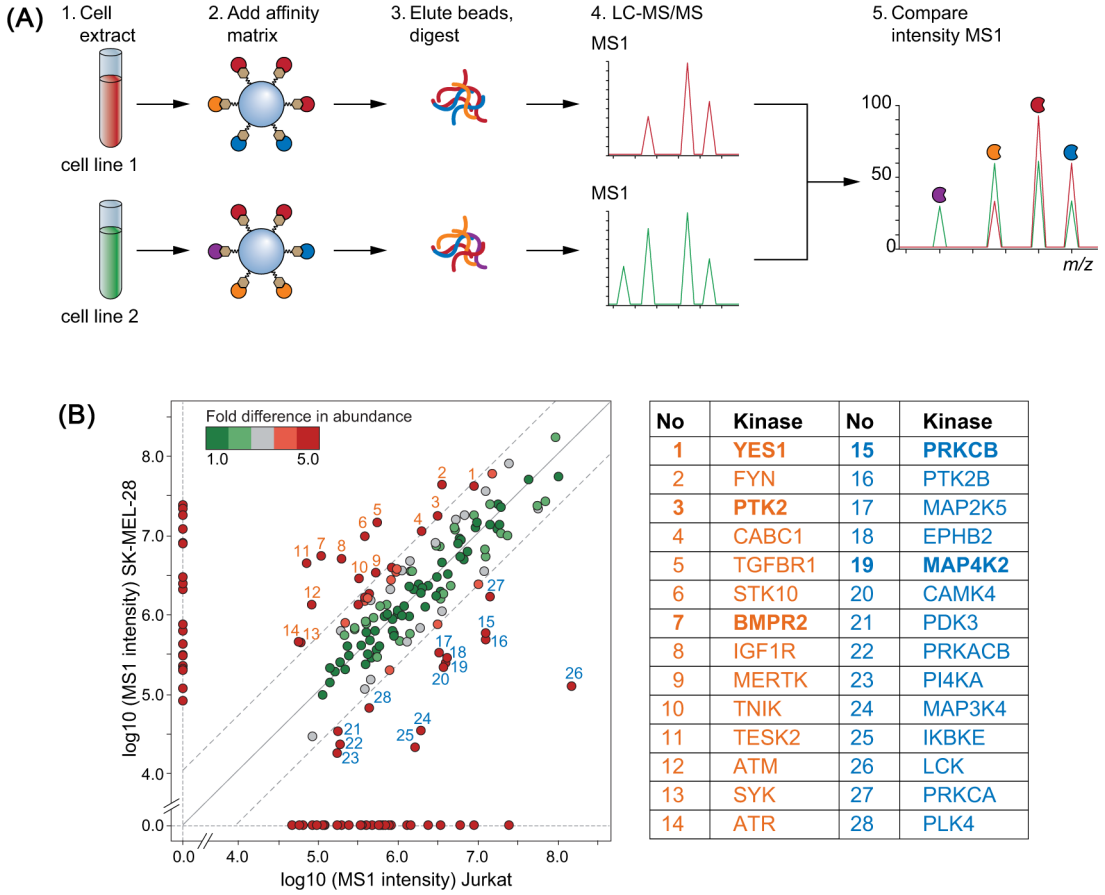

No	Kinase	No	Kinase
1	YES1	15	PRKCB
2	FYN	16	PTK2B
3	PTK2	17	MAP2K5
4	CABC1	18	EPHB2
5	TGFBR1	19	MAP4K2
6	STK10	20	CAMK4
7	BMPR2	21	PDK3
8	IGF1R	22	PRKACB
9	MERTK	23	PI4KA
10	TNIK	24	MAP3K4
11	TESK2	25	IKBKE
12	ATM	26	LCK
13	SYK	27	PRKCA
14	ATR	28	PLK4

Figure 1. Differential mapping of kinase expression between two cell lines. (A) Label-free protein quantification based on the intensity chromatograms of tryptic digests from full-scan mass spectral (MS1) data. Extracts from different cell types are incubated with kinobeads affinity matrix. After elution from the beads, samples are separated by SDS-PAGE, digested, and extracted. Tryptic peptides are sequenced by LC−MS/MS. Relative protein quantities are based on the three most abundant peptide ions (TOP3 method). (B) Differential mapping of kinase expression between Jurkat and SK-MEL-28 cell extracts determined as described in panel A. Each circle represents an identified kinase. Intensities of the topmost peptides intensities in the MS1 spectra (log10 scale) are shown; the color shows the fold change of abundances, where dark red labels a kinase that is >5-fold more or less abundant than in the other cell line, green = no difference in abundance. Red circles on the *x*- or *y*-axis are kinases that are identified in only one cell line (identified in Jurkat extract or SK-MEL28 extract, respectively). Kinases with strong difference in intensity are numbered and names are listed. For the kinases printed in boldface, IC_{50} curves are shown in Figure 2D.

affinities for the nucleotide cofactors ATP, ADP, and GTP across more than 200 kinases in two human cell lines, and demonstrate the potential impact of these profiles on inhibitor selectivity. The extensive kinase nucleotide binding data presented in this study represents a valuable resource for the assessment of target selectivity which is critical in kinase drug discovery.

RESULTS AND DISCUSSION

We previously described an affinity-based chemoproteomics strategy for the quantitative profiling of kinase inhibitors against a large fraction of the kinome in cell lines or primary cells. The method was based on an affinity matrix (kinobeads), which represents combinations of up to 8 immobilized small-molecule ATP-mimetics displaying differential selectivity across the human kinome. This affinity matrix captures kinases and related nucleotide-binding proteins from cell extracts *via* their ATP-binding sites. It can be used in a competition-binding assay format where free ligand or nucleotide added to the extract competes with the immobilized ligands for target binding, such that quantification of captured proteins by mass spectrometry allows the determination of ligand affinities.[9,27,28]

In the present study, we generated kinase-nucleotide affinity data for two human cell lines, Jurkat cells derived from T-cell lymphoma and SK-MEL-28 cells derived from melanoma. We employed two variations of the kinobeads competition assay that employ different sets of immobilized ligands optimized for the capturing of kinases from the ePK (eukaryotic protein kinase) and the aPK (lipid and related atypical kinases) family, as described previously.[9,28]

Differential Kinome Profile of Two Human Cell Lines.

We assessed to what degree nucleotide affinities determined in our experimental system would be dependent on the nature of the cell sources. We selected Jurkat cells and SK-MEL-28 cells, which differ in their growth properties (suspension *versus* adherent), relative kinase expression levels, and the major signaling pathways involved in transformation, *i.e.*, the PTEN/PI3K pathway in Jurkat cells and the Raf/MAP kinase pathway in SK-MEL-28 cells.[29,30] The differential absolute quantification of the kinobeads-captured subproteomes from the two cell types was performed by integrating extracted ion chromatograms of the three most abundant peptide ions per protein (TOP3 method),[31,32] thus enabling a high dynamic range of protein quantification (Figure 1A). We detected pronounced differences in protein kinase abundances between the two cell

dx.doi.org/10.1021/cb3005879 | *ACS Chem. Biol.* 2013, 8, 599−607

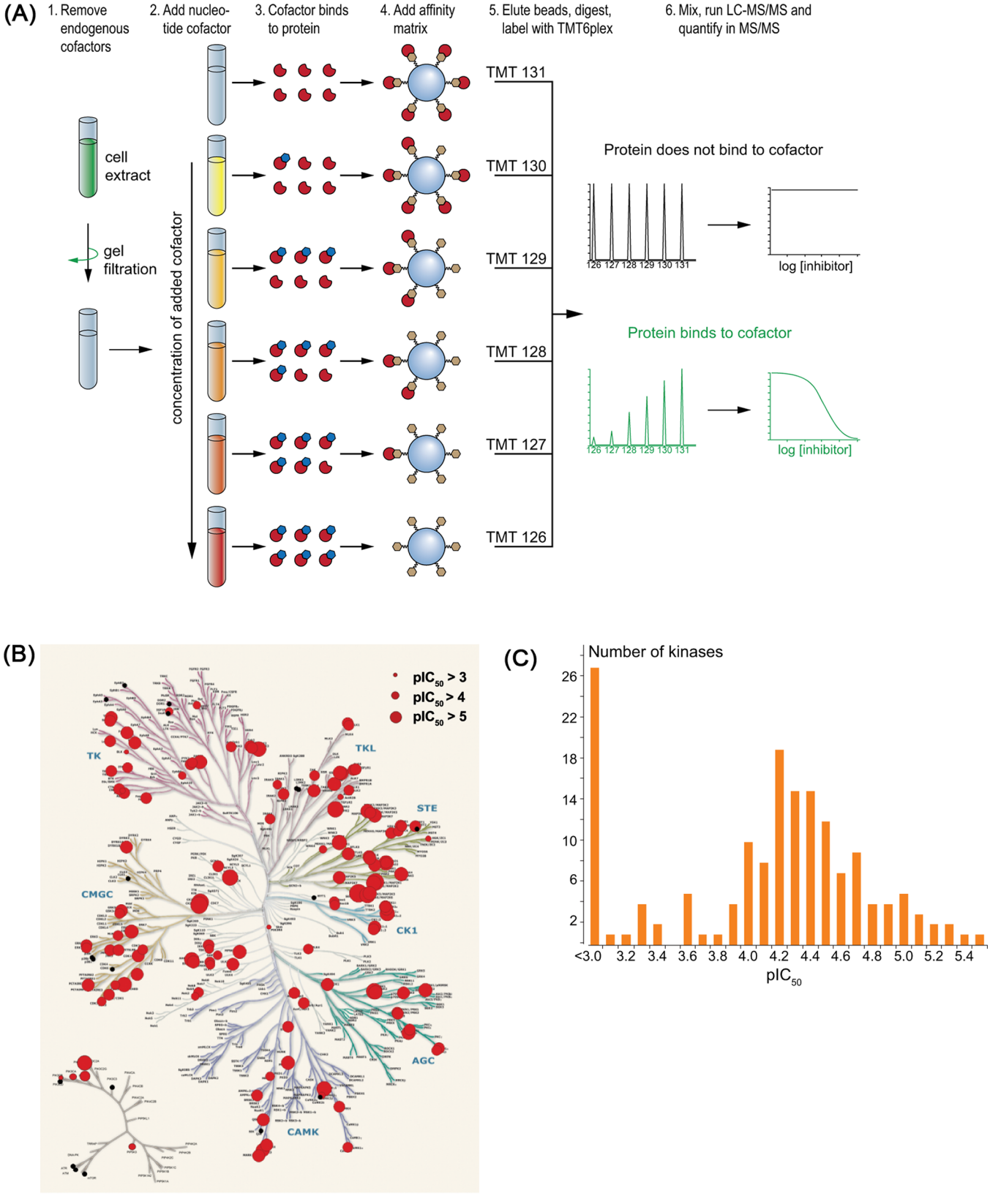

Figure 2. continued

dx.doi.org/10.1021/cb3005879 | *ACS Chem. Biol.* 2013, 8, 599–607

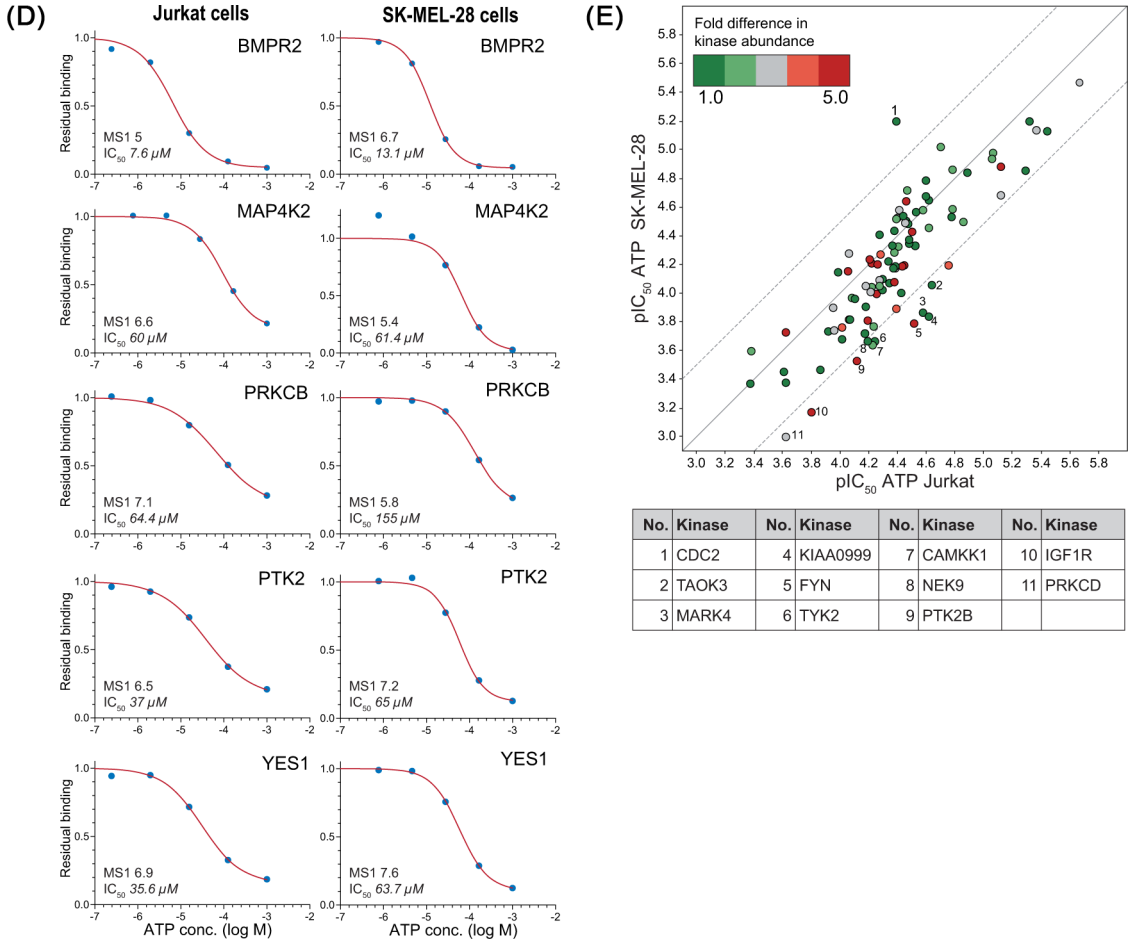

No.	Kinase	No.	Kinase	No.	Kinase	No.	Kinase
1	CDC2	4	KIAA0999	7	CAMKK1	10	IGF1R
2	TAOK3	5	FYN	8	NEK9	11	PRKCD
3	MARK4	6	TYK2	9	PTK2B		

Figure 2. Kinase-MgATP affinities are in the low micromolar to millimolar range. (A) Kinobeads nucleotide cofactor profiling workflow. Endogenous cofactors are removed using gel filtration before cell extracts are treated with control (buffer) or with nucleotide over a range of concentrations. Subsequently, proteins are captured on kinobeads. The free nucleotide competes with the immobilized ligands for nucleotide binding. Bound proteins are digested with trypsin and each peptide pool is labeled with TMT6-plex reagent. All six samples are combined and analyzed by LC−MS/MS. Each peptide gives rise to six characteristic TMT reporter signals (scaled to 100%) indicative of the nucleotide concentration used. For each peptide detected, the decrease of signal intensity compared to the vehicle control reflects competition by the free nucleotide for its target. (B) MgATP affinity (pIC_{50}) of Jurkat cell kinases displayed in the human kinome tree. Cell extracts were processed as outlined in panel A, and MgATP was spiked into cell extracts at concentrations ranging from 0.2 μM to 1 mM. Circles indicate pIC_{50} determined. (C) Distribution of MgATP pIC_{50} values for Jurkat cell kinases. Each bar represents the number of kinases identified with the indicated pIC_{50} (*x*-axis, bins of 0.1). Kinases not inhibited (*i.e.*, IC_{50} > 1 mM) are summed in the left bar. (D) Examples of IC_{50} curves for kinases that were identified with different abundances in Jurkat *versus* SK-MEL-28 cells (BMPR2, MAP4K2, PRKCB, PTK2, YES1). (E) Comparison of pIC_{50} for kinases identified from Jurkat cells (*x*-axis) and SK-MEL-28 cells (*y*-axis). The color code indicates kinase abundance differences between cell lines (allowing comparison with Figure 1B). The dashed lines are drawn at 3-fold difference. IC_{50} values appear to be largely independent of the cell source.

lines (Figure 1B and Supplementary Table S2a). Of a total of 201 kinases quantified, 146 were detected in both cell lines but frequently at different expression levels. Further, 21 were identified only from Jurkat and 34 from SK-MEL-28 cells. Notably, our kinase abundance results are in good agreement with published mRNA data (Supplementary Table S2b).[33]

ATP-Binding Properties of the Kinome in Jurkat and SK-MEL-28 Cells. For chemoproteomics profiling, whole cell extracts containing a nonionic, nondenaturing detergent (0.4% Nonidet P-40) were gel-filtered to remove endogenous nucleotides and other low molecular weight compounds and spiked with buffer without or with ATP in five concentrations ranging from 0.8 μM to 1 mM. Subsequently each sample was subjected to kinobeads affinity enrichment. During this step, the matrix-immobilized ATP-mimetics and the added free ATP compete for binding to the target proteins, such that ATP-binding proteins are precluded from binding to the affinity matrix in a concentration-dependent fashion. Proteins captured by the matrix were quantified by LC−MS/MS of the combined peptide pools from ATP-treated and untreated samples after six-plex peptide tandem-mass tagging (TMT).[34] For each peptide detected by MS/MS, the decrease of reporter ion signal intensity relative to the buffer control reflects binding of the protein to ATP (Figure 2A). We determined 6-point ATP-binding profiles for 163 kinases and found half-maximal inhibitory concentrations (IC_{50}) in the low micromolar to millimolar range. Profiling of ePK and aPK kinases was carried out in separate experiments utilizing different types of kinobeads matrix, and the results were aggregated for the affinity profiles (Figure 2B−D, and Supplementary Table S3, individual data for CZK2 and CZK73 experiments are reported in Data Set 2). Only two kinases, the casein kinase II isoforms CSNK2A1 and CSNK2A2, were captured by both types of kinobeads, notably with nearly identical IC_{50} values (Supple-

dx.doi.org/10.1021/cb3005879 | ACS Chem. Biol. 2013, 8, 599−607

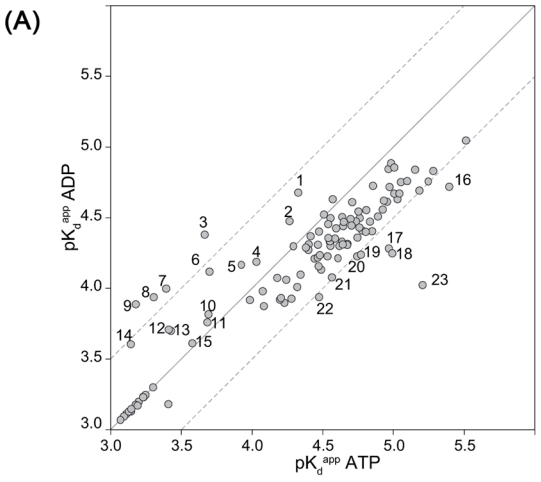

No	Kinase	No	Kinase
1	GAK	13	SIK2
2	PIK3CG	14	INSR
3	PIK3CA	15	PIP5K3
4	NEK2	16	MAP2K1
5	ABL2	17	MARK3
6	CAMK2G	18	PRKCQ
7	CAMK2D	19	MARK4
8	PKMYT1	20	MARK2
9	EPHA3	21	ACVR1
10	BLK	22	NEK9
11	PRKDC	23	MAP3K4
12	EPHB2		

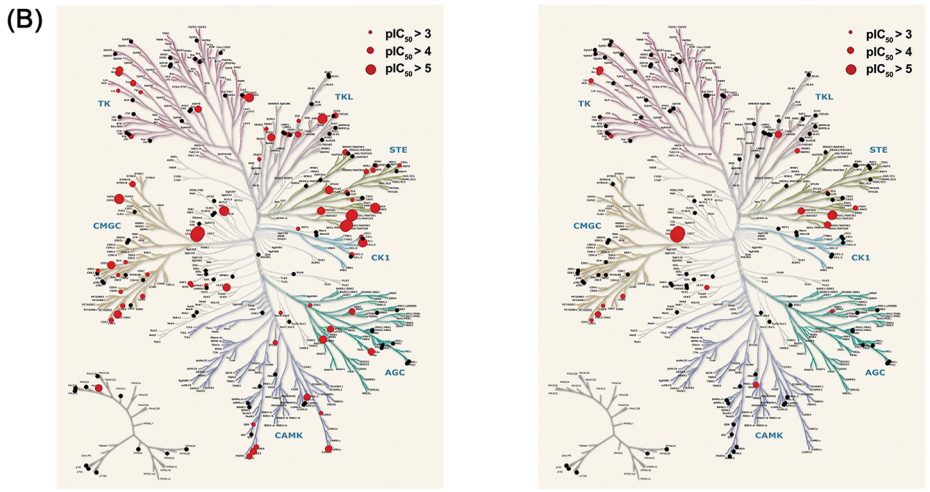

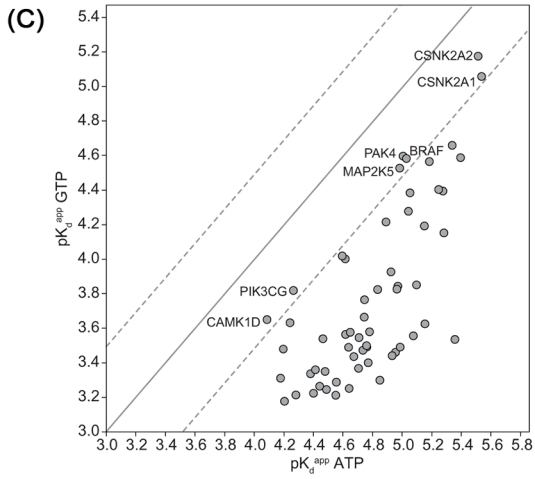

Figure 3. Kinases exhibit similar affinities for ATP and ADP, but only few kinases bind GTP. (A) Scatter plot of pK_d^{app} values for ATP and ADP; each circle represents a kinase; outer dashed lines show the 3-fold range of pK_d^{app} values. Kinases showing strong or different pK_d^{app} values (more than 3-fold lower or higher pK_d^{app} for ADP than for ATP) are labeled with numbers and names are listed in the table. The loss of the γ-phosphate group of ATP does not lead to a substantial loss in affinity. (B) GTP affinities for both cell lines, Jurkat and SK-MEL-28; each circle represents the pIC$_{50}$. Right and left panels show the pIC$_{50}$ in Jurkat extract or SK-MEL-28 extract, respectively. In both cell lines CSNK2A1/2 show high affinity for GTP. (C) Comparison of MgGTP and MgATP profile (Jurkat cell extract); each circle represents a kinase, where the *x*-axis or *y*-axis shows the pK_d^{app} for the nucleotide cofactor MgATP or MgGTP, respectively. All profiled kinases exhibited markedly lower affinity for GTP with the exception of CSNK2A1 and CSNK2A2, which showed similar high affinity for ATP and GTP.

mentary Data Set 2). However, the IC$_{50}$ values in this system may be affected by factors that cause the depletion of the target proteins from the extract, such as a high affinity of the kinase for the immobilized ligands and a low concentration of the kinase in the lysate.[9] Therefore, it is advantageous to determine the degree of depletion for each kinase, which allowed the calculation of apparent dissociation constants (K_d^{app}) values from the IC$_{50}$ values (Supplementary Figure S1a).[35] For most

dx.doi.org/10.1021/cb3005879 | *ACS Chem. Biol.* 2013, 8, 599–607

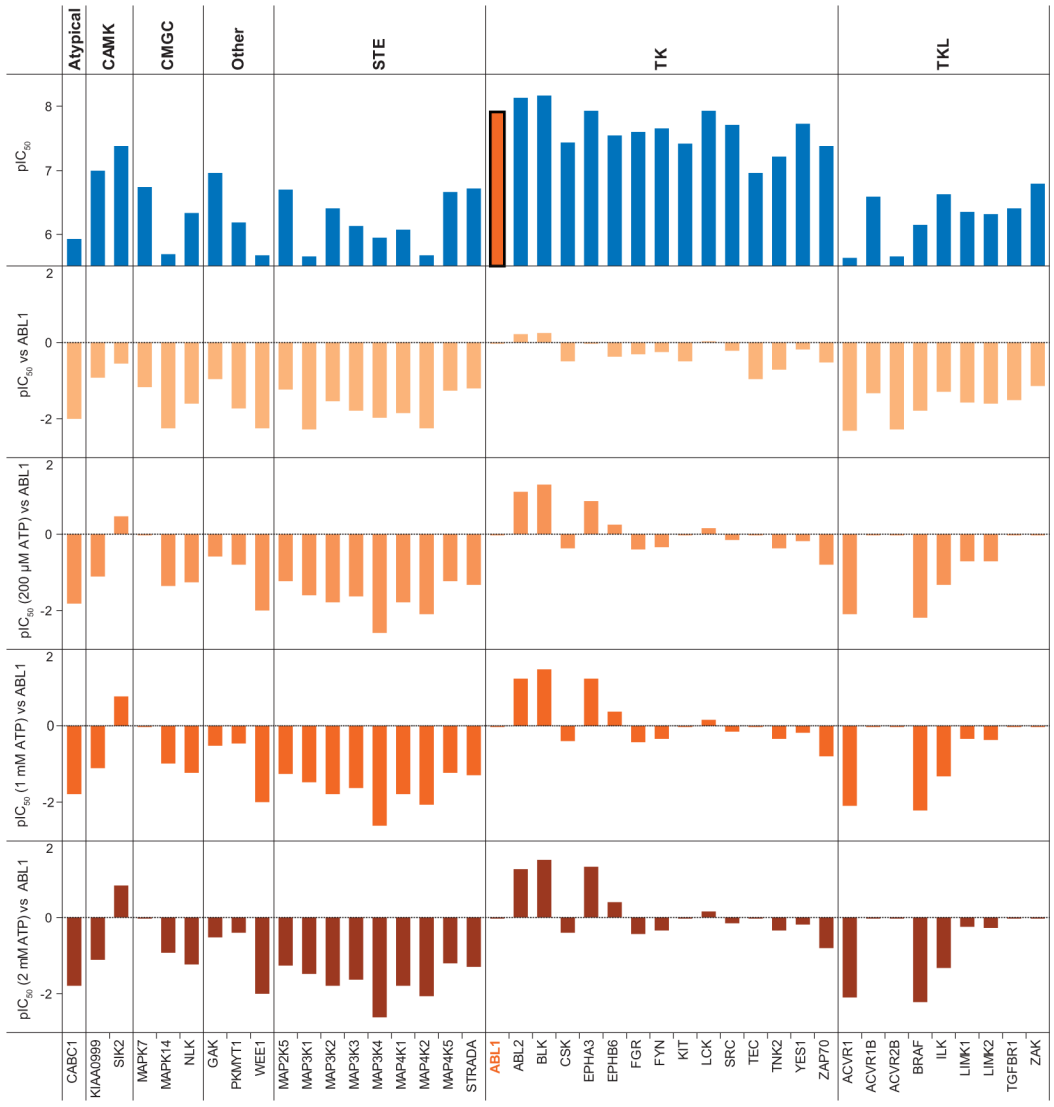

Figure 4. Differential kinase-ATP binding properties influence the selectivity of kinase drugs. To demonstrate how intracellular ATP affects the selectivity profile of a typical kinase inhibitor, pIC_{50} and pK_d^{app} values were determined for the tyrosine kinase drug dasatinib. Only kinases for which dasatinib exhibited a pIC_{50} value above 5.5 are shown. Using the pK_d^{app} values for ATP, the impact of the intracellular ATP concentration on the inhibitor IC_{50} value for each kinase was calculated using the Cheng−Prusoff relationship. Selectivity profiles are shown as dependent on the presence of 0.2, 1, and 2 mM ATP. Selectivity windows are represented relative to the drug's cognate target, ABL1 (marked in red).

kinases, we observed a low degree of depletion, resulting in a less than 3-fold deviation between K_d^{app} and IC_{50} values for 99% of the kinases (Supplementary Figure S1B and C, Supplementary Table S3 and S4). In order to assess to what degree the ATP-binding properties in our cell extract system are influenced by the cell source, we compared the ePK kinobeads results from Jurkat cells with data from an analogous experiment performed in SK-MEL-28 cells. For 97 kinases we were able to determine IC_{50} values for ATP in both cell lines. Notably, the IC_{50} values appeared to be largely independent of the cell source. We observed a few more pronounced differences (11 kinases differ more than 3-fold in IC_{50}), but these do not show any obvious correlation with differences in kinase expression levels (Figure 2D and E, compare with Figure 1B). Because tight binding of ATP might indicate a higher degree of structural similarity in the conformation of the ATP pocket, which has typically been observed for kinases in their active state,[36,37] we hypothesized whether there might be a correlation between the affinity of a given kinase for ATP and the frequency by which it shows up in inhibitor selectivity profiles. However, no such correlation was observed between the ATP affinities determined in this study and inhibitor "promiscuity" data taken from the currently most extensive public set of kinase inhibitor selectivity data (Supplementary Figure S2).[19]

Affinities for Other Nucleotide Cofactors: MnATP, ADP, and GTP. We further explored kinase-nucleotide binding in Jurkat cells by assessing the effect of replacing Mg^{2+} in our lysis buffer with Mn^{2+}, which is known to increase K_M for some kinases,[22] and profiled kinase affinities for ADP and GTP. We found that MnATP binds to most kinases with lower affinity than MgATP, with few exceptions where a moderate increase in affinity was observed (Supplementary Figure S3, Supplementary Table S3). The kinome affinity profile for ADP was generally in good agreement with the ATP profile, suggesting that the loss of the γ-phosphate group does not lead to a substantial loss in nucleotide affinity (Figure 3A, Supplementary Table S3). This result is consistent with observations that

dx.doi.org/10.1021/cb3005879 | ACS Chem. Biol. 2013, 8, 599−607

ADP release is frequently a time-limiting step in catalysis, and indeed product inhibition by ADP has been reported for some kinases.[22]

Very few kinases, including CK2, have been reported to utilize GTP in addition to ATP as cosubstrate.[38] Indeed, CK2 displayed the highest pK_d^{app} value in the GTP affinity kinobeads profile. In agreement with previous reports, we found that this kinase displayed only a slightly lower affinity for MgGTP compared to MgATP (Figure 3B, Supplementary Figure S3, Supplementary Table S3). In addition, we identified a few more kinases that displayed similar affinities for GTP and ATP, notably several MAP2K/MEK family members, BRAF, and PAK4 (Figure 3C). In order to test to what extent these kinases might utilize GTP as phosphate donor, we performed radiometric kinase assays for CK2, BRAF, and MAP2K1, utilizing purified recombinant enzymes and peptide or protein substrates. We found that only CK2 efficiently utilized GTP, whereas BRAF was very weakly active and MAP2K1 was inactive (Supplementary Figure S4). However, in the presence of ATP as phosphate donor, GTP exerted a small but significant activation of BRAF, similar to the transactivation mechanism that was reported to occur with low concentrations of inhibitors.[39] Notably, BRAF and MAP2K1, as well as PAK4, act in signaling pathways regulated by the Ras family of GTPases, and it is tempting to speculate that changes in the local concentration of GTP might also impact directly on these kinases by acting as an endogenous inhibitor or activator.

Differential ATP-Binding Properties Influence the Selectivity of Kinase Drugs. A particular advantage of our kinobeads-based strategy is that kinase affinities for a given small molecule inhibitor and for ATP can be assessed in the same cell extract system, and the resulting data can be combined to generate a profile, which more accurately predicts selectivity in the presence of excess ATP, which is typically present in the cell at low millimolar concentrations. We examined the selectivity profile of the leukemia drug dasatinib, an inhibitor of the ABL and SRC tyrosine kinases. The kinobeads-derived profile of dasatinib in Jurkat cells showed that, out of a total of 140 kinases, the compound inhibited 20 kinases with a K_d^{app} below 100 nM, *i.e.*, within a ~10-fold selectivity window of its target ABL (K_d^{app} = 10 nM). The IC_{50} value of a cell-penetrant compound in the presence of competing cellular ATP may be approximated by $IC_{50}^{int} \approx K_d^{app}\,(1 + ([ATP])/(K_d^{app}{}_{ATP}))$,[40] which impacts the selectivity windows according to the degree that each target kinase is affected by competition from intracellular ATP (Figure 4, Supplementary Table S5). Based on the kinase-ATP affinities determined in this study, selectivity windows with respect to ABL change in the presence of ATP such that 8 kinases fall within the 10-fold range, with SIK2 and the Eph kinases EphB2, EphA3, and EphB6 now dominating the target profile.

In conclusion, we have substantially extended our kinobeads-based chemoproteomics strategy for kinase inhibitor profiling. We demonstrated that apparent ligand affinities determined in this complex system are not substantially affected by kinase expression levels and, for the majority of kinases, are consistent across two different cell types. Because our approach does not depend on the optimization of assay variables for individual enzymes, we were able to determine affinities for cellular nucleotide cofactors, most importantly the kinase cosubstrate ATP, for a large number of kinases under a single defined set of experimental conditions. Knowledge of the ATP affinity for each kinase in a given selectivity profile allows a more accurate prediction of potency and selectivity in cell-based systems, which is expected to contribute to the optimization of compound selectivity early in the discovery process, leading to reduced attrition at later stages.

METHODS

Chemoproteomics Profiling. Reagents were purchased from Sigma unless otherwise noted. Cell lines were purchased from ATCC and cultured in RPMI1640 supplemented with 4.5 g/L glucose, 10 mM Hepes, 1 mM sodium pyruvate, and 10% fetal calf serum (FCS). Cell extracts were prepared as described[34] in lysis buffer (50 mM Tris/HCl pH 7.5, 5% (w/v) glycerol, 1.5 mM $MgCl_2$, 150 mM NaCl, 25 mM NaF, 1 mM sodium vanadate supplemented with 0.8% (w/v) NP-40 and EDTA-free protease inhibitor tablets (Roche)). Cell extract aliquots were gel filtered on PD10 columns (GE Healthcare) to remove cellular ATP and other nucleotides.[24] Separation was controlled by spectrophotometric analysis of fractions at 254 nm. It cannot be excluded that a fraction of nucleotides is "trapped" by protein, but this fraction is small as indicated by the fact that we determined IC_{50} values below 4 μM (*i.e.*, 4 μM ATP added back to the extract reduced capturing of CK2 by half). Each experiment is denoted by an identifier (ID) number. Supplemental Table 1 lists all experiments including experimental variables. IC_{50} values were determined in competition-binding assays.[9,34] Briefly, MgATP, MnATP, MgADP, or MgGTP was added to cell extracts in five concentrations (dilution series of 1:8 or 1:6, resulting in concentration ranges from 1 mM to 0.77 μM and from 1 mM to 0.24 μM, respectively) and incubated at 4 °C for 45 min. Two variations of kinobeads were prepared as described previously immobilizing combinations of ligands optimized for ePK[9] or aPK[28] family kinases. Experiments with ePK- and aPK-directed kinobeads were performed in parallel, utilizing aliquots of the same extract. Beads (35 μL per sample) were equilibrated in lysis buffer, incubated with 1 mL (5 mg protein) cell extract, transferred to disposable columns (MoBiTec), washed with lysis buffer containing 0.2% NP-40, and eluted with 50 μL 2x SDS sample buffer, supplemented with DTT. Proteins were alkylated with iodoacetamide, separated on 4−12% NuPAGE (Invitrogen), and stained with colloidal Coomassie. For the determination of dissociation constants (K_d^{app}), protein depletion was determined in a parallel experiment where a second aliquot of cell extract was incubated with kinobeads, and the nonbound fraction was subjected to a second incubation with fresh beads (Supporting Information, Figure S1).

MS Sample Preparation. Gels were sliced across the entire separation range and subjected to in-gel digestion with trypsin. Peptide extracts were labeled with TMT6plex (Thermo-Fisher Scientific) in 40 mM triethylammoniumbicarbonate, pH 8.5. After quenching of the reaction with glycine, labeled peptide pools were combined. Peptides were optionally prefractionated using reversed phase chromatography at pH 12, dried, and resuspended in 0.1% formic acid in water.

LC−MS/MS and Data Analysis. Aliquots of the sample were injected into a nano-LC system (Eksigent 1D+) coupled to LTQ-Orbitrap mass spectrometers (Thermo-Finnigan). Peptides were separated on custom 50 cm × 75 μM (internal diameter) reversed-phase columns (Reprosil) at 40 °C. Gradient elution was performed from 2% acetonitrile to 40% acetonitrile in 0.1% formic acid over 2−4.5 h. Intact peptides were detected in the Orbitrap at 30.000 resolution. Internal calibration was performed using the ion signal from $(Si(CH_3)_2O)6H+$ at m/z 445.1200252. Data-dependent tandem mass spectra were generated for up to six peptide precursors using a combined CID/HCD approach, using HCD at a resolution of 7,500 with a 70% normalized collision energy. For CID, up to 5,000 ions (Orbitrap XL) were accumulated in the ion trap within a maximum ion accumulation time of 200 ms. For HCD, target ion settings were 50,000 (Orbitrap XL). The experiments were performed using an inclusion list for kinase peptides as previously described.[41] MGF files were created and submitted to the Mascot 2.0 (Matrix Science) search engine, using 10 ppm mass tolerance for peptide precursors and 0.8 Da (CID) tolerance for fragment ions. Search parameter settings include

dx.doi.org/10.1021/cb3005879 | ACS Chem. Biol. 2013, 8, 599−607

carbamidomethylation of cysteine residues and TMT modification of lysine residues as fixed modifications and methionine oxidation, N-terminal acetylation of proteins, and TMT modification of peptide N-termini as variable modifications. A 2.5 mDa mass tolerance was used for TMT reporter ion extraction in HCD scans by in-house-developed software. Only peptides unique for identified proteins and present on the inclusion lists were used for relative protein quantification. Only proteins identified with >1 peptide and >2 spectra were reported in this study. For the comparison of kinase abundance in two cell lines, MS1 intensities were extracted from the vehicle-treated aliquots used in the IC_{50} profiling experiments. XICs were matched to identified peptides. The apex of the XIC peak had to be located within 30 s from the time of the MS/MS event performed on the peptide in question. The raw intensities of the XICs of the peptides with identical sequences were summed (*i.e.*, same sequence, but different charge states and/or different modifications), and the resulting single entity was referred to as a sequence. For each protein the 3 sequences with the highest raw XIC intensity from a given sample were selected and log10 transformed.[32] These values were then summed, and the mean was calculated. In cases where fewer than 3 sequences were associated, the mean was calculated on 2 or 1 sequences. Of the identified kinases from both Jurkat and SK-MEL-28 cells, the 10 most abundant were used to normalize for MS instrument differences. In order to avoid a substantial deviation of IC_{50} values from true affinities, it is advantageous to use sufficient amounts of cell extract such that depletion of proteins from the extract is limited.[9] This can be ensured by the experimental determination of protein depletion.[35] One aliquots of cell extract was incubated with the affinity matrix, and captured proteins were eluted, digested, and labeled with TMT6plex. A second aliquot of cell extract was also incubated with the affinity matrix, and the nonbound fraction was subjected to a second incubation with fresh matrix. From this second incubation the bound proteins were likewise eluted, digested, and labeled. The ratio r of the target bound in the second incubation *versus* target bound in first incubation was calculated, where $1 - r$ represents the depletion factor applied. Supplementary Data sets 1–3 include all data for MS1 comparison, affinity profiles and correction factors.

■ ASSOCIATED CONTENT

Supporting Information

This material is available free of charge *via* the Internet at http://pubs.acs.org.

■ AUTHOR INFORMATION

Corresponding Author

*E-mail: marcus.x.bantscheff@gsk.com; gerard.c.drewes@gsk.com.

Author Contributions

I.B. conducted biochemical experiments and performed mass spectrometry; M.S. and M.F.S. performed data analysis and visualization; C.H. contributed ideas and supported the work; M.B. and G.D. planned and supervised research and wrote the paper.

Notes

The authors declare the following competing financial interest(s): The authors are employees of Cellzome GmbH, a GlaxoSmithKline company, which funded the work.

■ ACKNOWLEDGMENTS

We would like to thank J.-I. Huber and K. Weis for cell culture; B. Dümpelfeld, M. Klös-Hudak, and T. Rudi for sample preparation,; N. Zinn and M. Boesche for operating LC–MS instrument;, and F. Weisbrodt for preparing figures. We are grateful to O. Rausch for discussions and advice.

■ REFERENCES

(1) Cohen, P. (2002) Protein kinases—the major drug targets of the twenty-first century? *Nat. Rev. Drug Discovery 1*, 309–15.

(2) Fedorov, O., Muller, S., and Knapp, S. (2010) The (un)targeted cancer kinome. *Nat. Chem. Biol. 6*, 166–169.

(3) Manning, G., Whyte, D. B., Martinez, R., Hunter, T., and Sudarsanam, S. (2002) The protein kinase complement of the human genome. *Science 298*, 1912–34.

(4) Zhang, J., Yang, P. L., and Gray, N. S. (2009) Targeting cancer with small molecule kinase inhibitors. *Nat. Rev. Cancer 9*, 28–39.

(5) Grant, S. K. (2009) Therapeutic protein kinase inhibitors. *Cell. Mol. Life Sci. 66*, 1163–1177.

(6) Fabbro, D., Cowan-Jacob, S. W., Mobitz, H., and Martiny-Baron, G. (2012) Targeting cancer with small-molecular-weight kinase inhibitors. *Methods Mol. Biol. 795*, 1–34.

(7) Cohen, P. (2009) Targeting protein kinases for the development of anti-inflammatory drugs. *Curr. Opin. Cell Biol. 21*, 317–324.

(8) Huang, D., Zhou, T., Lafleur, K., Nevado, C., and Caflisch, A. (2010) Kinase selectivity potential for inhibitors targeting the ATP binding site: a network analysis. *Bioinformatics 26*, 198–204.

(9) Bantscheff, M., Eberhard, D., Abraham, Y., Bastuck, S., Boesche, M., Hobson, S., Mathieson, T., Perrin, J., Raida, M., Rau, C., Reader, V., Sweetman, G., Bauer, A., Bouwmeester, T., Hopf, C., Kruse, U., Neubauer, G., Ramsden, N., Rick, J., Kuster, B., and Drewes, G. (2007) Quantitative chemical proteomics reveals mechanisms of action of clinical ABL kinase inhibitors. *Nat. Biotechnol. 25*, 1035–1044.

(10) Karaman, M. W., Herrgard, S., Treiber, D. K., Gallant, P., Atteridge, C. E., Campbell, B. T., Chan, K. W., Ciceri, P., Davis, M. I., Edeen, P. T., Faraoni, R., Floyd, M., Hunt, J. P., Lockhart, D. J., Milanov, Z. V., Morrison, M. J., Pallares, G., Patel, H. K., Pritchard, S., Wodicka, L. M., and Zarrinkar, P. P. (2008) A quantitative analysis of kinase inhibitor selectivity. *Nat. Biotechnol. 26*, 127–132.

(11) Huang, D., Zhang, Y., and Chen, X. (2003) Analysis of intracellular nucleoside triphosphate levels in normal and tumor cell lines by high-performance liquid chromatography. *J. Chromatogr., B: Anal. Technol. Biomed. Life Sci. 784*, 101–109.

(12) Traut, T. W. (1994) Physiological concentrations of purines and pyrimidines. *Mol. Cell. Biochem. 140*, 1–22.

(13) Knight, Z. A., and Shokat, K. M. (2005) Features of selective kinase inhibitors. *Chem. Biol. 12*, 621–637.

(14) Force, T., and Kolaja, K. L. (2011) Cardiotoxicity of kinase inhibitors: the prediction and translation of preclinical models to clinical outcomes. *Nat. Rev. Drug Discovery 10*, 111–126.

(15) Anastassiadis, T., Deacon, S. W., Devarajan, K., Ma, H., and Peterson, J. R. (2011) Comprehensive assay of kinase catalytic activity reveals features of kinase inhibitor selectivity. *Nat. Biotechnol. 29*, 1039–1045.

(16) Bain, J., McLauchlan, H., Elliott, M., and Cohen, P. (2003) The specificities of protein kinase inhibitors: an update. *Biochem. J. 371*, 199–204.

(17) Bain, J., Plater, L., Elliott, M., Shpiro, N., Hastie, C. J., McLauchlan, H., Klevernic, I., Arthur, J. S., Alessi, D. R., and Cohen, P. (2007) The selectivity of protein kinase inhibitors: a further update. *Biochem. J. 408*, 297–315.

(18) Davies, S. P., Reddy, H., Caivano, M., and Cohen, P. (2000) Specificity and mechanism of action of some commonly used protein kinase inhibitors. *Biochem. J. 351*, 95–105.

(19) Davis, M. I., Hunt, J. P., Herrgard, S., Ciceri, P., Wodicka, L. M., Pallares, G., Hocker, M., Treiber, D. K., and Zarrinkar, P. P. (2011) Comprehensive analysis of kinase inhibitor selectivity. *Nat. Biotechnol. 29*, 1046–1051.

(20) Fabian, M. A., Biggs, W. H., III, Treiber, D. K., Atteridge, C. E., Azimioara, M. D., Benedetti, M. G., Carter, T. A., Ciceri, P., Edeen, P. T., Floyd, M., Ford, J. M., Galvin, M., Gerlach, J. L., Grotzfeld, R. M., Herrgard, S., Insko, D. E., Insko, M. A., Lai, A. G., Lelias, J. M., Mehta, S. A., Milanov, Z. V., Velasco, A. M., Wodicka, L. M., Patel, H. K., Zarrinkar, P. P., and Lockhart, D. J. (2005) A small molecule-kinase interaction map for clinical kinase inhibitors. *Nat. Biotechnol. 23*, 329–336.

(21) Goldstein, D. M., Gray, N. S., and Zarrinkar, P. P. (2008) High-throughput kinase profiling as a platform for drug discovery. *Nat. Rev. Drug Discovery 7*, 391−397.
(22) Schwartz, P. A., and Murray, B. W. (2011) Protein kinase biochemistry and drug discovery. *Bioorg. Chem. 39*, 192−210.
(23) Breitkopf, S. B., Oppermann, F. S., Keri, G., Grammel, M., and Daub, H. (2010) Proteomics analysis of cellular imatinib targets and their candidate downstream effectors. *J. Proteome Res. 9*, 6033−6043.
(24) Patricelli, M. P., Nomanbhoy, T. K., Wu, J., Brown, H., Zhou, D., Zhang, J., Jagannathan, S., Aban, A., Okerberg, E., Herring, C., Nordin, B., Weissig, H., Yang, Q., Lee, J. D., Gray, N. S., and Kozarich, J. W. (2011) In situ kinase profiling reveals functionally relevant properties of native kinases. *Chem. Biol. 18*, 699−710.
(25) Bantscheff, M., and Drewes, G. (2012) Chemoproteomic approaches to drug target identification and drug profiling. *Bioorg. Med. Chem. 20*, 1973−1978.
(26) Rix, U., and Superti-Furga, G. (2009) Target profiling of small molecules by chemical proteomics. *Nat. Chem. Biol. 5*, 616−624.
(27) Kruse, U., Pallasch, C. P., Bantscheff, M., Eberhard, D., Frenzel, L., Ghidelli, S., Maier, S. K., Werner, T., Wendtner, C. M., and Drewes, G. (2011) Chemoproteomics-based kinome profiling and target deconvolution of clinical multi-kinase inhibitors in primary chronic lymphocytic leukemia cells. *Leukemia 25*, 89−100.
(28) Bergamini, G., Bell, K., Shimamura, S., Werner, T., Cansfield, A., Muller, K., Perrin, J., Rau, C., Ellard, K., Hopf, C., Doce, C., Leggate, D., Mangano, R., Mathieson, T., O'Mahony, A., Plavec, I., Rharbaoui, F., Reinhard, F., Savitski, M. M., Ramsden, N., Hirsch, E., Drewes, G., Rausch, O., Bantscheff, M., and Neubauer, G. (2012) A selective inhibitor reveals PI3Kgamma dependence of T(H)17 cell differentiation. *Nat. Chem. Biol. 8*, 576−582.
(29) Conner, S. R., Scott, G., and Aplin, A. E. (2003) Adhesion-dependent activation of the ERK1/2 cascade is by-passed in melanoma cells. *J. Biol. Chem. 278*, 34548−34554.
(30) Xu, Z., Stokoe, D., Kane, L. P., and Weiss, A. (2002) The inducible expression of the tumor suppressor gene PTEN promotes apoptosis and decreases cell size by inhibiting the PI3K/Akt pathway in Jurkat T cells. *Cell Growth Differ. 13*, 285−296.
(31) Grossmann, J., Roschitzki, B., Panse, C., Fortes, C., Barkow-Oesterreicher, S., Rutishauser, D., and Schlapbach, R. (2010) Implementation and evaluation of relative and absolute quantification in shotgun proteomics with label-free methods. *J. Proteomics 73*, 1740−1746.
(32) Silva, J. C., Gorenstein, M. V., Li, G. Z., Vissers, J. P., and Geromanos, S. J. (2006) Absolute quantification of proteins by LCMSE: a virtue of parallel MS acquisition. *Mol. Cell Proteomics 5*, 144−156.
(33) Wu, C., Orozco, C., Boyer, J., Leglise, M., Goodale, J., Batalov, S., Hodge, C. L., Haase, J., Janes, J., Huss, J. W., III, and Su, A. I. (2009) BioGPS: an extensible and customizable portal for querying and organizing gene annotation resources. *Genome Biol. 10*, R130.
(34) Bantscheff, M., Hopf, C., Savitski, M. M., Dittmann, A., Grandi, P., Michon, A. M., Schlegl, J., Abraham, Y., Becher, I., Bergamini, G., Boesche, M., Delling, M., Dumpelfeld, B., Eberhard, D., Huthmacher, C., Mathieson, T., Poeckel, D., Reader, V., Strunk, K., Sweetman, G., Kruse, U., Neubauer, G., Ramsden, N. G., and Drewes, G. (2011) Chemoproteomics profiling of HDAC inhibitors reveals selective targeting of HDAC complexes. *Nat. Biotechnol. 29*, 255−265.
(35) Sharma, K., Weber, C., Bairlein, M., Greff, Z., Keri, G., Cox, J., Olsen, J. V., and Daub, H. (2009) Proteomics strategy for quantitative protein interaction profiling in cell extracts. *Nat. Methods 6*, 741−744.
(36) Huse, M., and Kuriyan, J. (2002) The conformational plasticity of protein kinases. *Cell 109*, 275−82.
(37) Johnson, L. N. (2009) Protein kinase inhibitors: contributions from structure to clinical compounds. *Q. Rev. Biophys. 42*, 1−40.
(38) Niefind, K., Putter, M., Guerra, B., Issinger, O. G., and Schomburg, D. (1999) GTP plus water mimic ATP in the active site of protein kinase CK2. *Nat. Struct. Biol. 6*, 1100−1103.
(39) Poulikakos, P. I., Zhang, C., Bollag, G., Shokat, K. M., and Rosen, N. (2010) RAF inhibitors transactivate RAF dimers and ERK signalling in cells with wild-type BRAF. *Nature 464*, 427−430.
(40) Cheng, Y., and Prusoff, W. H. (1973) Relationship between the inhibition constant (K1) and the concentration of inhibitor which causes 50% inhibition (I50) of an enzymatic reaction. *Biochem. Pharmacol. 22*, 3099−3108.
(41) Savitski, M. M., Fischer, F., Mathieson, T., Sweetman, G., Lang, M., and Bantscheff, M. (2010) Targeted data acquisition for improved reproducibility and robustness of proteomic mass spectrometry assays. *J. Am. Soc. Mass Spectrom. 21*, 1668−1679.